Relativistic and correlation effects in atoms

B. P. Das, K. V. P. Latha, Bijaya K. Sahoo, Chiranjib Sur, Rajat K Chaudhuri
Atomic and Molecular Physics Group, Indian Institute of Astrophysics, Bangalore - 560 034, India
and
D. Mukherjee
Indian Association for the Cultivation of Science, Kolkata - 700 032, India

2nd February 2008

Abstract

This review article deals with some case studies of relativistic and correlation effects in atomic systems. After a brief introduction to relativistic many-electron theory, a number of applications ranging from correlation energy to parity non-conservation in atoms are considered. There is a special emphasis on relativistic coupled-cluster theory as most of the results presented here are based on it.

Key words : Relativistic electronic structure and coupled-cluster theory

1 Introduction

One of the most important milestones in the development of theoretical atomic physics has been the formulation and application of theories that can simultaneously treat relativistic and correlation effects in atoms. Following the early work of Swirles on relativistic Hartree-Fock or Dirac-Fock (DF) theory [1], Grant made pioneering contributions to the numerical and angular momentum aspects of this theory [2] which paved the way for further advances in the field. Multi-configuration Dirac-Fock (MCDF) [3, 4] and relativistic many-body perturbation theory (RMBPT) [5] codes were developed in the mid 1970s and early 1980s calculations based on them soon followed [6, 7, 8, 9]. During the 1980s and 1990s, these two theories were applied to a wide range of atoms and ions to study a variety of properties [10, 11, 12, 13]. The extension of coupled-cluster theory to the relativistic regime during the last decade is indeed a very significant development [14]. Linear and non-linear versions of this theory have been successfully used in performing high precision calculations of a number of different atomic properties [15, 16, 17, 18].

The present review is by no means comprehensive; it mainly highlights some of the work on relativistic and correlation effects in atoms undertaken in our group. Unlike molecules, a number of different relativistic many-body calculations have been carried out on atoms using a variety of methods. Relativistic many-body calculations on atoms are currently much more advanced than those on molecules [19, 20, 21, 22]. In addition to the inclusion of the Breit interaction, certain types of QED effects have also been included in atomic calculations. It will take several years before molecular calculations reach this level of sophistication. Relativistic many-body calculations of parity and time reversal violations in some atoms have been performed to an accuracy of better than 1%. These calculations in combination with accurate experiments are now poised to test the Standard Model (SM) of particle physics. It is not clear at the present time whether it would be possible to achieve something comparable from studies on discrete symmetry violations of molecules.

The organization of the paper is as follows : Section 2 deals with the Dirac-Coulomb approximation and the section following it (section 3), touches upon the Breit interaction and QED effects. Section 4 is an overview of relativistic coupled-cluster theory which has been used in the majority of the calculations considered here. In section 5, we present the basic ideas underlying two physical effects that are relativistic in origin – fine-structure splitting and permanent electric dipole moment of atoms arising from the electric dipole moment of an electron and have given the results of some representative calculations. The enhancement of relativistic effects in heavy atoms along with the influence of electron correlation is discussed in section 6 with reference to correlation energy, hyperfine interactions and parity non-conservation in atoms. In the last section we make some concluding remarks.

2 The Dirac-Coulomb Approximation

For an N-electron atom, the relativistic Hamiltonian is given by

$$H = \sum_{i=1}^{N} \left[c\vec{\alpha_i} \cdot \vec{p_i} + \beta mc^2 + V_N(r_i) \right] + \sum_{i<j}^{N} \frac{e^2}{r_{ij}}\,, \tag{1}$$

where α and β are given by $\alpha_i = \begin{pmatrix} 0 & \sigma_i \\ \sigma_i & 0 \end{pmatrix}$ and $\beta = \begin{pmatrix} I & 0 \\ 0 & -I \end{pmatrix}$; σ_i are the Pauli matrices and I represents the unit matrix. $V_N(r_i)$ is the nuclear potential at the site of the ith electron and the last term is the Coulomb interaction between the electrons. H defined above is known as Dirac-Coulomb Hamiltonian which is clearly not covariant.

This Hamiltonian can also be written as

$$H = \sum_{i} h_0(i) + \sum_{i<j} \frac{e^2}{r_{ij}}\,. \tag{2}$$

The electron-electron interaction can be approximated by an average potential where each electron moves independently in an average field caused by the nucleus and the other electron. This is the independent particle model which is the starting point of most atomic physics calculations. This can be put into a mathematical footing by partitioning the full Hamiltonian in the following way :

$$H = H_0 + V_{es}, \tag{3}$$

where

$$H_0 = \sum_{i}^{N} h_0(i) \tag{4}$$

is a sum of the one electron operators,

$$h_0(i) = c\alpha_i \cdot p_i + \beta mc^2 + U(r_i). \tag{5}$$

It is customary to assume U as the Dirac-Fock potential [23] and

$$V_{es} = -\sum_{i} U(r_i) + \sum_{i<j} \frac{e^2}{r_{ij}} \tag{6}$$

can be treated as a perturbation if there are no strongly interacting configurations in the system. The many-body atomic state $|\Psi(\Gamma, J, M)\rangle$ is an eigen function of the Dirac-Coulomb Hamiltonian and satisfies the equation,

$$H|\Psi(\Gamma, J, M)\rangle = E|\Psi(\Gamma, J, M)\rangle, \tag{7}$$

where J, M are the total angular momentum quantum numbers and Γ is the quantum number which distinguishes each of the atomic states. These states are expanded in terms of the determinantal wavefunctions which in turn are built from the single particle orbitals. If $|\Phi(\Gamma, J, M)\rangle$'s denote the determinantal wavefunctions, then,

$$|\Psi(\Gamma, J, M)\rangle = \sum_{k} C_k |\Phi_k(\Gamma, J, M)\rangle. \tag{8}$$

The coefficients C_ks are determined by the choice of the theory. The single particle orbitals are the two-component Dirac spinors,

$$|\phi_{n\kappa m}\rangle = \frac{1}{r} \begin{pmatrix} P_{n\kappa}(r)\chi_{\kappa m} \\ iQ_{n\kappa}(r)\chi_{-\kappa m} \end{pmatrix}, \tag{9}$$

where n and m are the principal quantum number and magnetic quantum number respectively. κ is a quantum number given by

$$\kappa = \begin{cases} l & \text{for } j = l - \frac{1}{2} \\ -(l+1) & \text{for } j = l + \frac{1}{2} \end{cases}, \tag{10}$$

where l is the orbital angular momentum and j is the total angular momentum of an electron.

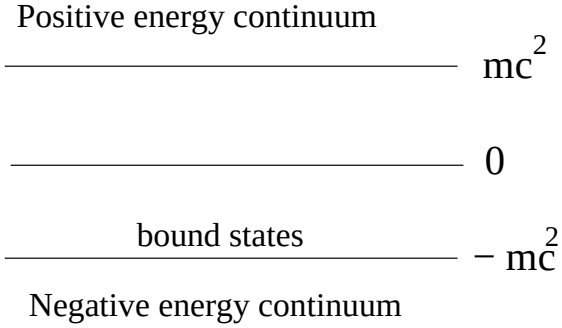

Figure 1: Positive and negative energy states

The solutions of the Dirac equation admit both positive and negative energy states [23] and this is shown in figure 1. For a free particle, only continuum states exist above $mc^2$and below $-mc^2$. However, electrons in an atom that are acted on by a relativistic mean-field potential in addition to continuum states above mc^2 and below $-mc^2$bound states do exist in the interval $-mc^2$ and mc^2. The variational principle fails due to the presence of negative energy states [24]. The radial parts of the large and small components of the Dirac spinor are expanded in terms of Gaussian functions [25] as follows

$$P_{n\kappa}(r) = \sum_i C^L_{\kappa i} g^L_{\kappa i}(r),$$

$$Q_{n\kappa}(r) = \sum_i C^S_{n\kappa} g^S_{\kappa i}(r), \tag{11}$$

where S and L stands for small and large component respectively and the g's are Gaussian type functions of the form

$$g^L_{\kappa i}(r) = C^L_N r^{n_\kappa} \exp(-\alpha_i r^2). \tag{12}$$

In the case of finite basis set expansions the condition of kinetic balance is applied to prevent the variational collapse [26]. The kinetic balance condition [24, 27, 28] gives the relation between the large and small component of radial wave function as follows :

$$g^S_{\kappa i}(r) = C^S_N \left(\frac{d}{dr} + \frac{\kappa}{r} \right) g^L_{\kappa i}(r). \tag{13}$$

In Eq. (12) and (13) C^L_N and C^S_N are the normalization factors for the large and small components respectively.

3 Beyond the Dirac-Coulomb Approximation

The electron-electron interaction can be treated relativistically, by including corrections to the Coulomb interaction. The leading relativistic correction to the Coulomb interaction is the Breit interaction [29], where the interaction Hamiltonian is given by,

$$H_B = -e^2 \sum_{i<j} \frac{\alpha_i \cdot \alpha_j}{r_{ij}} + \frac{(\alpha_i \cdot r_{ij})\,(\alpha_j \cdot r_{ij})}{r^3_{ij}}. \tag{14}$$

Here the matrices α_i, α_j are built from the Dirac matrices and r_{ij} is the inter-electronic distance. The magnitude of the Breit interaction is smaller than that of the Coulomb interaction by a factor α^2, where α is the fine structure constant and it can be included perturbatively or self consistently [30]. In addition to the Breit interaction, inclusion of QED effects like the self-energy and the vacuum polarization [31] may be necessary for an accurate quantitative description of certain properties where relativistic effects are important.

The process involving the emission and absorption of a virtual photon by the same electron is known as self-energy. According to Dirac's theory, the vacuum consists of a homogeneous sea of negative-energy

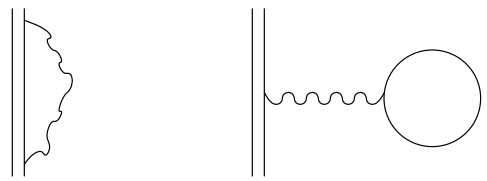

Figure 2: Corrections to Coulomb interaction

electrons. A bound electron in the atom can interact with an electron in the Dirac sea, thereby changing the charge distribution of the negative energy electrons compared to the free-field case. This results in the creation of electron-positron pairs and hence the vacuum behaves as a polarizable medium. This process is known as vacuum polarization. Figure 2 illustrates the self-energy and the vacuum polarization processes [32].

Only a few calculations of self energy and the vacuum polarization (which together give rise to the Lamb shift) have been performed on many electron atoms. As the Coulomb interaction due to the nucleus is much stronger than the electron-electron interactions in the inner shells of heavy atoms, it is reasonable to calculate the Lamb shift for such systems using the hydrogenic or screened hydrogenic approximation [33]. More sophisticated calculations of QED effects have been carried out in the past few years. The details of these calculations can be found in a review article by Shabaev [34].

4 Relativistic Coupled Cluster Theory : An overview

In this section we will briefly introduce the relativistic coupled cluster theory; one of the most powerful and accurate relativistic many-body theories. It is equivalant to all order relativistic many-body perturbation theory and has the virtue of being size-extensive [35]. Most of the work described in the subsequent section are based on this theory.

We start with the DF state $|\Phi\rangle$ built out of four component orbitals given by Eq. (9), as the Fermi vacuum, and then the normal ordered Hamiltonian can be expressed as

$$H_N \equiv H - \langle\Phi| H |\Phi\rangle = H - E_{DF}, \tag{15}$$

where H is the Dirac-Coulomb Hamiltonian.

If we project $\langle\Phi|\exp(-T)$ from the left we obtain the correlation energy (ΔE) and if we project any of the excited determinant $\langle\Phi^\star|\exp(-T)$ we additionally get a set of equations which are used to obtain the T amplitudes. Using the normal ordered dressed Hamiltonian $\overline{H}_N = \exp(-T)H_N\exp(T)$ the corresponding equations for correlation energy and amplitudes become

$$\langle\Phi|\overline{H}_N|\Phi\rangle = \Delta E, \tag{16}$$

and

$$\langle\Phi^\star|\overline{H}_N|\Phi\rangle = 0. \tag{17}$$

Here the state $|\Phi^\star\rangle$ may be singly excited $|\Phi_a^r\rangle$ or double excited $|\Phi_{ab}^{rs}\rangle$ and so on. The indices $a, b, \cdots$ refer to holes and $p, q, \cdots$ to particles. We have considered the coupled cluster single and double (CCSD) approximation, where the cluster operator T is composed of one- and two-body excitation operators, *i.e.* $T = T_1 + T_2$, and are expressed in second quantization form

$$T = T_1 + T_2 = \sum_{ap}\left\{a_p^\dagger a_a\right\} t_a^p + \frac{1}{2}\sum_{abpq}\left\{a_p^\dagger a_q^\dagger a_b a_a\right\} t_{ab}^{pq}. \tag{18}$$

Contracting the ladder operators [36] and rearranging the indices, the amplitude equations can be expressed in the form

$$A + B(T)\cdot T = 0, \tag{19}$$

where A is a vector consisting of the matrix elements $\langle\Phi^\star|\, H_N\, |\Phi\rangle$ and T is the vector representing the excitation amplitudes and $B(T)$ is the matrix which depends on the cluster amplitudes so that Eq. (19) is solved self-consistently. For example, a typical contribution to the term $\overbrace{\overbrace{H_N T_2} T_2}$ is

$$B_{ab}^{pq} = \frac{1}{2}\sum_{dgrs} V_{dgrs} t_{ad}^{pr} t_{gb}^{sq}. \tag{20}$$

Here V_{dgrs} is the two-electron Coulomb integral and t_{ad}^{pr} is the cluster amplitude corresponding to a simultaneous excitation of two electrons from orbital a and d to p and r respectively. Diagrammatic techniques are used to obtain all the terms which contribute to this specific contribution.

For an atom with one valance electron we first compute the correlations for the closed shell system, *i.e.* singly ionized atom using the closed shell coupled cluster approach. The reference state for the open shell system is

$$\left|\Phi_k^{N+1}\right\rangle \equiv a_k^\dagger \left|\Phi\right\rangle \tag{21}$$

with the particle creation operator $a_k^\dagger$. Then by using the excitation operators for both the core and valance electron the exact state is defined as [37]:

$$\left|\Psi_k^{N+1}\right\rangle = \exp(T)\left\{\exp(S_k)\right\}\left|\Phi_k^{N+1}\right\rangle. \tag{22}$$

Here $\{\exp(S_k)\}$ is the normal ordered exponential representing the valance part of the wave operator. Here

$$S_k = S_{1k} + S_{2k} = \sum_{k\neq p}\left\{a_p^\dagger a_k\right\} s_k^p + \sum_{bpq}\left\{a_p^\dagger a_q^\dagger a_b a_k\right\} s_{kb}^{pq}, \tag{23}$$

where k stands for valance orbital. S_k contain the particle annihilation operator a_k, and because of the normal ordering it cannot be connected to any other valance electron excitation operator and so $\{\exp(S_k)\}$ automatically reduces to $(1+S_k)$.

Then we can write the Eq.(22) as

$$\left|\Psi_k^{N+1}\right\rangle = \exp(T)\left(1+S_k\right)\left|\Phi_k^{N+1}\right\rangle, \tag{24}$$

and obtain a set of equations [36]

$$\left\langle\Phi_k^{N+1}\right|\overline{H}_N\left(1+S_k\right)\left|\Phi_k^{N+1}\right\rangle = H_{eff} \tag{25}$$

and

$$\left\langle\Phi_k^{\star N+1}\right|\overline{H}_N\left(1+S_k\right)\left|\Phi_k^{N+1}\right\rangle = H_{eff}\left\langle\Phi_k^{\star N+1}\right|\left(1+S_k\right)\left|\Phi_k^{N+1}\right\rangle. \tag{26}$$

The Eq.(26) is non-linear in S_k because H_{eff} is itself a function of S_k. Hence, these equations have to solved self-consistently to determine the S_k amplitudes.

The normalized transition matrix element $(i \longrightarrow f)$ due to an operator $\widehat{O}$ is given by

$$\begin{aligned}\widehat{O}_{fi} &= \frac{\left\langle\Psi_f^{N+1}\right|\widehat{O}\left|\Psi_i^{N+1}\right\rangle}{\sqrt{\left\langle\Psi_f^{N+1}\right|\left.\Psi_f^{N+1}\right\rangle\left\langle\Psi_i^{N+1}\right|\left.\Psi_i^{N+1}\right\rangle}} \\ &= \frac{\left\langle\Phi_f^{N+1}\right|\left\{1+S_f^\dagger\right\}\exp(T^\dagger)\widehat{O}\exp(T)\{1+S_i\}\left|\Phi_i^{N+1}\right\rangle}{\sqrt{\left\langle\Phi_f^{N+1}\right|\left\{1+S_f^\dagger\right\}\exp(T^\dagger)\exp(T)\{1+S_f\}\left|\Phi_f^{N+1}\right\rangle\left\langle\Phi_i^{N+1}\right|\left\{1+S_i^\dagger\right\}\exp(T^\dagger)\exp(T)\{1+S_i\}\left|\Phi_i^{N+1}\right\rangle}},\end{aligned} \tag{27}$$

whereas the expectation value of any operator $\widehat{O}$ can be written as the normalized form with respect to the exact state $\left|\Psi^{N+1}\right\rangle$ as

$$\left\langle\widehat{O}\right\rangle = \frac{\left\langle\Psi^{N+1}\right|\widehat{O}\left|\Psi^{N+1}\right\rangle}{\left\langle\Psi^{N+1}\right|\left.\Psi^{N+1}\right\rangle} = \frac{\left\langle\Phi^{N+1}\right|\left\{1+S^\dagger\right\}\exp(T^\dagger)\widehat{O}\exp(T)\left\{1+S\right\}\left|\Phi^{N+1}\right\rangle}{\left\langle\Phi^{N+1}\right|\left\{1+S^\dagger\right\}\exp(T^\dagger)\exp(T)\left\{1+S\right\}\left|\Phi^{N+1}\right\rangle}. \tag{28}$$

Table 1: Fine structure intervals for B-like ions in cm^{-1}.

Z	Dirac-Fock (DF)	Dirac-Coulomb (DC)	Breit	QED	Total	Experiment
20	37581.8	38119	-1616	124	36627	36615(30)
22	57678.6	58319	-2241	180	56258	56243(4)
24	84973.2	85715	-3015	251	82951	829926(20)
26	121045.8	121898	-3958	341	118281	118266(20)
28	167653.8	168635	-5092	451	163994	163961(50)
30	226739.4	227889	-6437	586	222038	

5 Purely relativistic effects

5.1 Fine-Structure splitting

The fine-structure splitting is relativistic in origin, but is influenced by electron correlation. It occurs between the states having same values of the total orbital quantum number L, total spin quantum number S and different total angular momentum J. There have been many attempts to calculate this quantity for a variety of atoms in their ground and excited states [38]. We present here the interesting case of the ground state fine structure splitting of boron which has been calculated by different relativistic approaches [39, 40, 41]. Boron is an open-shell atom with the configuration $1s^2 2s^2 2p^1$. The relativistic configuration interaction method (CI) was used by Das *et al* [41]. The single particle orbitals used in the calculations there were obtained by the application of the variational principle. Consider an energy functional given by

$$\varepsilon = \sum_r a_r \langle \Phi_r | H | \Phi_r \rangle \tag{29}$$

where H is the Dirac-Coulomb Hamiltonian, $|\Phi_r\rangle$is the rth configuration state function (CSF) and a_r is given by

$$a_r = \frac{2J_r + 1}{\sum_s (2J_s + 1)}\,; \tag{30}$$

J_r and J_s being the total angular momenta of the rth and sth CSFs respectively. Minimization of ε with respect to the single particle orbitals ϕ_i,

$$\frac{\partial \varepsilon}{\partial \phi_i} = 0 \tag{31}$$

yields a set of differential equations which were solved self-consistently by using an appropriate numerical method [42]. In this calculation, all relativistic configurations arising from $1s^2 2s^2 2p^1$, $1s^2 2s^2 2p^2$and $1s^2 2p^3$ were considered. The Breit interaction and QED effects (self-energy and vacuum polarization in the hydrogenic approximation) were treated as first order perturbations. We give below the results of the calculation. The electron correlation contributions (difference of Dirac-Coulomb+Breit and Dirac-Fock) vary from -1078.8 to -5287.4 for $Z = 20$ to $Z = 30$. It is the evident from table.1 that the Breit interaction and the QED effects play an important role and their inclusion is critical in obtaining good agreement with experiments.

5.2 Electric Dipole Moment of the electron

The presence of a non-zero electric dipole moment (EDM) on a non-degenerate physical system would be a direct evidence of Parity ($\hat{P}$) and Time-reversal ($\hat{T}$) symmetry violations. An atom can have a non-zero EDM due to a non-zero EDM of it's constituent electron, under certain conditions. According to a theorem by Schiff, in 1963 [43], *the EDM of an atom vanishes even if it's constituents have non-vanishing EDMs*. This theorem was based on the following assumptions :

1. the constituents of the atoms are non-relativistic particles,
2. the interactions between the particles in an atom are electrostatic,
3. the EDM distribution of each atomic constituent coincides with its charge distribution.

By considering the relativistic effects in atoms, Sandars showed that an atom can have a non-zero EDM [44]. If an electron has a non-zero EDM d_e, the relativistic interaction of d_e with the internal electric field of the atom, is given by,

$$H_I = -\sum_i d_e \beta_i \vec{\sigma}_i \cdot \vec{E}_i^{int}, \tag{32}$$

where E^{int} is the electric filed inside the atom; $\vec{\sigma}_i$ are Pauli matrices and β is Dirac matrix defined in section 2. This reduces to,

$$H_I = -\sum_i d_e \vec{\sigma}_i \cdot \vec{E}_i^{int} \tag{33}$$

in the non-relativistic limit. It is possible to express the relativistic form of H_I in terms of an effective one particle Hamiltonian, given by [45]

$$H_I = 2ic\beta_i \gamma_i^5 p_i^2 \,, \tag{34}$$

where c is the velocity of light, $\gamma_5 = i\gamma_0\gamma_1\gamma_2\gamma_3$ and $\gamma_i = \beta\alpha_i$. The Schrödinger equation for the unperturbed state $|\Psi_\alpha^{(0)}\rangle$ is

$$H_0|\Psi_\alpha^{(0)}\rangle = E_\alpha^{(0)}|\Psi_\alpha^{(0)}\rangle \,, \tag{35}$$

where $|\Psi_\alpha^{(0)}\rangle = \exp(T^{(0)})|\Phi_\alpha^{(0)}\rangle$ in coupled-cluster theory and H_0 is the Dirac-Coulomb Hamiltonian.

In the presence of EDM interaction, which is treated as a perturbation, the Schrödinger equation becomes

$$H|\Psi_\alpha\rangle = E_\alpha|\Psi_\alpha\rangle \,, \tag{36}$$

where $H = H_0 + \lambda H_I$ and $|\Psi_\alpha\rangle = \exp(T^{(0)} + \lambda T^{(1)})|\Phi_\alpha^{(0)}\rangle$. Here $T^{(0)}$and $T^{(1)}$are the unperturbed and perturbed cluster amplitudes and the perturbation parameter, $\lambda = d_e$. The $T^{(0)}$and $T^{(1)}$amplitudes are determined from the following equations :

$$\langle\Phi^\star|\,\overline{H}_N\,|\Phi\rangle = 0 \tag{37}$$

and

$$\langle\Phi^\star|\left[\overline{H}_N, T^{(1)}\right]|\Phi_\alpha^{(0)}\rangle = -\langle\Phi^\star|\,\overline{H_I}|\Phi_\alpha^{(0)}\rangle. \tag{38}$$

The atomic EDM is given by,

$$d_A = \frac{\langle\Psi_\alpha|\vec{D}|\Psi_\alpha\rangle}{\langle\Psi_\alpha|\Psi_\alpha\rangle} = 0 \tag{39}$$

for non-relativistic case. $\vec{D}$ is the electric dipole operator. The enhancement factor R is given by,

$$R = \frac{d_a}{d_e} = \frac{\langle\Psi_\alpha^{(0)}|\vec{D}|\Psi_\alpha^{(1)}\rangle + \langle\Psi_\alpha^{(1)}|\vec{D}|\Psi_\alpha^{(0)}\rangle}{\langle\Psi_\alpha^{(0)}|\Psi_\alpha^{(0)}\rangle} \tag{40}$$

Following Coupled Cluster theory the equation (Eq. 40) reduces to

$$R = \frac{\langle\Phi_0|T^{(1)^\dagger}\vec{D} + \vec{D}T^{(1)}|\Phi_0\rangle}{\langle\Phi_0|\Phi_0\rangle} \,. \tag{41}$$

An alternative Coupled Cluster approach to EDMs is given by Shukla et al [46]. The values of d_e predicted by various models of particle physics are given in table 2.

The current best limit on the electron EDM comes from the Tl measurement [47]. The enhancement factor atomic thallium to the electron EDM $R = -585$, which is based on relativistic coupled-cluster calculation [48]. Comparing with experiment, the limit on the electron EDM is

$$d_e \leq 1.6 \times 10^{-27}\text{e-cm}. \tag{42}$$

The enhancement factor for atomic Cs (Z=55) has been obtained as $R = 130.5$ from a method combining RMBPT and the MCDF approach [49]. The calculation done by Martensson *et al* [50] gives $R = 114(1 \pm 0.03)$ for Cs.

Table 2: Value of d_e predicted by various models of particle physics

Model	$d_e$in $e-cm$
Standard Model	$< 10^{-38}$
Supersymmetric	$10^{-26} - 10^{-28}$
Multi-Higgs	$10^{-26} - 10^{-28}$
Left-right asymmetric	$10^{-26} - 10^{-28}$

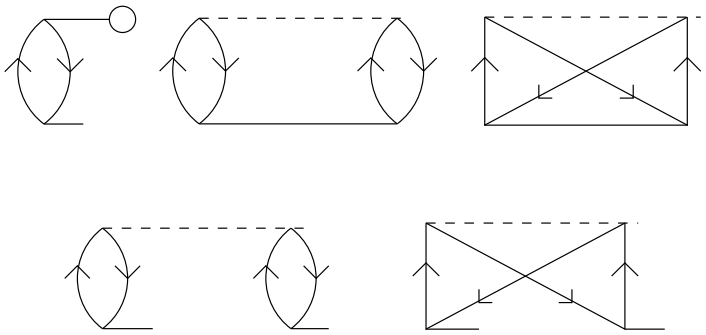

Figure 3: Diagrams contributing to correlation energy

6 Relativistic enhancements

6.1 Correlation energy

In the frame work of coupled-cluster theory, the expression for the correlation energy of an atom is given by,

$$E_{corr} = \langle \Phi | \bar{H}_N | \Phi \rangle, \tag{43}$$

where $\bar{H}_N = e^{-T} H_N e^T$ where H is the Dirac-Coulomb Hamiltonian described in section 2.

The diagrams given in figure 3 contribute to the correlation energy, where the dotted lines represent the coulomb interaction between the electrons, the solid line corresponds to the cluster operator T and the circle represents the one-electron operator.

We have computed the above expression for the correlation energy using the coupled-cluster wave-functions for the closed-shell atoms, Xe^{54}, Yb^{70} and Hg^{80}. The results are shown in table 3.

From the above results it is clear that with the increase in the atomic number (Z), the relativistic effects become more prominent. The absolute magnitude of the Dirac-Fock contribution hence increases and that of the correlation energy decreases for xenon, ytterbium and mercury.

The orbitals used in the calculation are expanded in terms of Gaussian functions of the type [51]

$$F_{i,k}(r) = r^k \exp(-\alpha_i r^2), \tag{44}$$

with $k = 0, 1, 2 \cdots$ for $s, p, d, \cdots$ type functions, respectively. The exponents are determined by the even tempering condition [52]

Table 3: Comparison of correlation and Dirac-Fock energy

Atom	Dirac Fock energy	δE_{corr}
Xe^{54}	-0.74474960061E+04	-0.71694286411
Yb^{70}	-0.14069217432E+05	-0.56956394691
Hg^{80}	-0.19650686115E+05	-0.44792843655

Table 4: Details of the basis used in the calculation

symmetry	Total basis in each symmetry	No. of excited orbitals	α_0 and β used
$s_{1/2}$	13	8	0.00725 ; 2.725
$p_{1/2}$	11	7	0.00755 ; 2.755
$p_{3/2}$	11	7	0.00755 ; 2.755
$d_{3/2}$	8	2	0.00775 ; 2.765
$d_{5/2}$	8	2	0.00775 ; 2.765
$f_{5/2}$	5	5	0.00780 ; 2.805
$f_{7/2}$	5	5	0.00780 ; 2.805
$g_{7/2}$	3	3	0.00785 ; 2.825
$g_{9/2}$	3	3	0.00785 ; 2.825

$$\alpha_i = \alpha_0 \beta^{i-1}. \tag{45}$$

The values of $\alpha_0$and β for different symmetries are given in table 4.

6.2 Hyperfine interaction

A nucleus may possess electromagnetic multipole moments, which can interact with the electromagnetic field produced by the electrons at the site of the nucleus . The interaction between various moments of the nucleus and the electrons of an atom are collectively known as hyperfine interactions [37]. This interaction produce shifts of the electronic energy levels which are usually much smaller than those corresponding to the fine structure splittings.

The non-vanishing moments are the magnetic multipole moments for odd k and electric multipole moments for even k. The most important of these moments is the magnetic dipole moment ($k = 1$) which is associated with the nuclear spin. The interaction of this particular moment with the electron is known as magnetic dipole hyperfine interaction.

In general the hyperfine interaction is given by [53]

$$H_{hfs} = \sum_k M^{(k)} \cdot T^{(k)}, \tag{46}$$

where $M^{(k)}$ and $T^{(k)}$ are spherical tensors of rank k, which corresponds to nuclear and electronic parts of the interaction respectively.
For the magnetic dipole hyperfine interaction [54]

$$T_q^{(1)} = \sum_q t_q^{(1)} = \sum_j -ie\sqrt{\frac{8\pi}{3}} \frac{\overrightarrow{\alpha_j}}{r_j^2} \cdot \mathbf{Y}_{1q}^{(0)}(\widehat{r_j}), \tag{47}$$

where $\overrightarrow{\alpha}$ is the Dirac matrix and $\mathbf{Y}_{kq}^{\lambda}$ is the vector spherical harmonics. In Eq.(47) the index j refers to the j-th electron of the atom and e is the magnitude of the electronic charge. The magnetic dipole hyperfine constant A is defined as

$$A = \mu_N \left(\frac{\mu_I}{I}\right) \frac{\langle J \| T^{(1)} \| J \rangle}{\sqrt{J(J+1)(2J+1)}}, \tag{48}$$

where μ_N is the nuclear Bohr magneton, μ_I is the nuclear magnetic moment, I is the nuclear spin, J is the total electronic angular momentum.

In Eq.(47) $t^{(1)}$ is the single particle reduced matrix element of $T^{(1)}$. The reductions of the single particle matrix element into angular factors and radial integral can be obtained by using the Wigner Eckart theorem. This single particle reduced matrix element is given by

$$\langle \kappa \| t^{(1)} \| \kappa' \rangle = - \langle \kappa \| C^{(1)} \| \kappa' \rangle (\kappa + \kappa') \int dr \frac{(P_\kappa Q_{\kappa'} + Q_\kappa P_{\kappa'})}{r^2}, \tag{49}$$

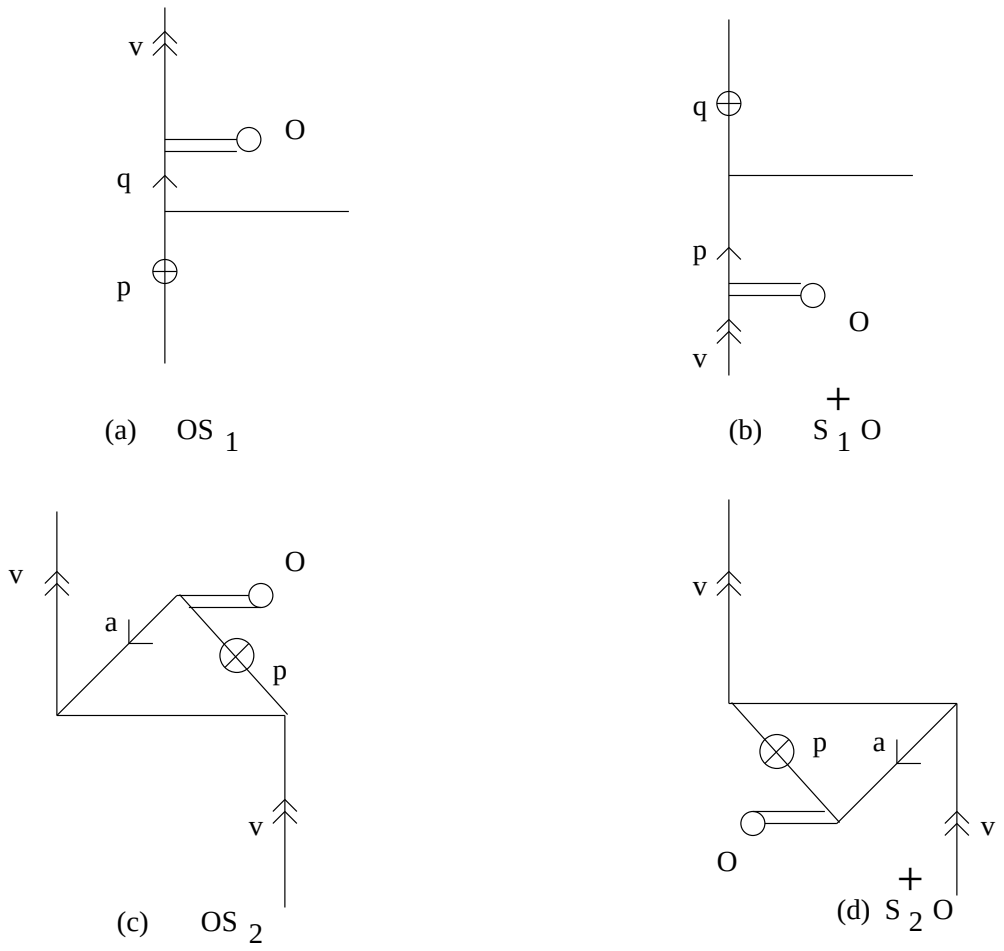

Figure 4: Goldstone diagrams for pair correlation (a,b) and core-polarization effects (c,d). Here a denotes a hole whereas v denotes valance orbital and $p, q, r...$ denote virtual orbitals (particles). The superscripts refer to the order of perturbation and the dashed lines correspond to the Coulomb interaction. Particles and holes (labeled by a) are denoted by the lines directed upward and downward respectively. The double line represents the O (the hyperfine interaction operator) vertices. The valance (labeled by v) and virtual orbitals (labeled by $p, q, r..$) are depicted by double arrow and single arrow respectively, whereas the orbitals denoted by $\oplus$ can either be valance or virtual.

where $\langle\kappa\| C^{(k)} \|\kappa'\rangle$ is the reduced matrix element of the Racah tensor and is equal to

$$(-1)^{j+1/2}\sqrt{(2j+1)(2j'+1)}\begin{pmatrix} j & k & j' \\ \frac{1}{2} & 0 & -\frac{1}{2} \end{pmatrix}\pi(l,k,l'),$$

with

$$\pi(l,k,l') = \begin{cases} 1 & \text{if } l+k+l' \text{ even} \\ 0 & \text{otherwise} \end{cases} .$$

Here the single particle orbitals are expressed in terms of the Dirac spinors with P_i and Q_i as large and small components respectively.

In the calculation for Ba^+we have used hybrid basis functions which are partly numerical and partly analytical [55]. The analytical orbitals have the form of Eq. (44). In table 5 the values of the magnetic dipole hyperfine constant (A) is given in MHz for $^{25}Mg^+$[56] and $^{137}Ba^+$ [57] for ground and one low lying excited state. In table 6 we have presented the contributions from Dirac-Fock (DF), pair correlation (PC) and core polarization (PC) effects.

It can be seen from this table (table 6) that for Mg^+ the CP contribution is larger than the PC in magnitude for both the states. It is important to note that the former contribution includes the hyperfine interaction of all the core orbitals while only a specific valence orbital is involved in this interaction for the

Table 5: Values of magnetic dipole hyperfine constant (A) in MHz for $^{25}Mg^{+}$and $^{137}Ba^{+}$

Atom		Theory	Experiment	Others
$^{25}Mg^{+}$	States			
	$3s_{1/2}$	592.86	596.25	602(8) [58]
				597.45 [59]
	$3p_{1/2}$	101.70		103.4 [59]
$^{137}Ba^{+}$				
	$6s_{1/2}$	4072.83	4018	4203.200 [60]
	$6p_{1/2}$	736.98	742.04	

Table 6: Contribution of pair correlation (PC) and core polarization (CP) effect in magnetic dipole hyperfine constant (A) in MHz

Atom		Dirac-Fock	PC	CP
$^{25}Mg^{+}$[56]	States			
	$3s_{1/2}$	468.819	39.713	77.767
	$3p_{1/2}$	77.975	7.293	15.153
$^{137}Ba^{+}$[57]				
	$6s_{1/2}$	2929.41	663.20	465.91
	$6p_{1/2}$	492.74	126.53	98.98

latter (see Fig. 4). However, the hyperfine constant A for Ba^{+} exhibits exactly the opposite behaviour. Even though Ba^{+} has more core electrons than Mg^{+}, the relativistic enhancement of the valence ($6s$) magnetic dipole hyperfine interaction results in the value of PC exceeding that of CP.

In table 7 we present the values of A for $6p\,^2P_{1/2}$ and $6p\,^2P_{3/2}$ states of Pb^{+}. The Dirac-Fock values for these two states deviate from their experimental values in opposite direction, suggesting that the signs of the correlation contributions are opposite for the two cases. This is evident from the result of our second order relativistic many-body perturbation theory (RMBPT(2)) calculation. Electron correlation is dramatic in the case of the $6p\,^2P_{3/2}$ state because of the large and negative core polarization (-840.6 MHz). However, the value of A at this level differs from experiment by 48%. After carrying out a RCCSD(T) calculation this discrepancy reduces to less than 7% . The agreement of the ground state value of A with experiment is about 0.7%. These calculations highlight the power of the relativistic coupled-cluster theory to account for the interplay of relativistic and correlation effects in systems with strongly interacting configurations [62].

6.3 Parity non-conservation in atoms to neutral weak interaction

The parity transformation can be expressed as $\overrightarrow{r} \longrightarrow -\overrightarrow{r}$ and the action of the parity operator $\hat{P}$ is given by

$$\hat{P}\psi(\overrightarrow{r}) = \psi(-\overrightarrow{r})\,, \tag{50}$$

where $\psi(\overrightarrow{r})$ is the wavefunction of a physical system. Parity conservation means that the system is invariant under parity transformation and the Hamiltonian H commutes with the parity operator, i.e. if H_P is the parity transformed Hamiltonian

Table 7: Magnetic dipole hyperfine constant for $6p$ states of Pb^+: a strongly interacting system. RMBPT(2) stands for second order RMBPT. Both RMBPT and RCCSD calculations are performed by our group.

States	$6p\,^2P_{1/2}$	$6p\,^2P_{3/2}$
Dirac-Fock	11513.5	918.4
RMBPT(2)	15722.5	302.9
RCCSD(T)	12903.7	623.2
Experiment [61]	13000	583(21)

$$H_p = \hat{P} H \hat{P}^{-1} = H$$

and therefore

$$\left[H, \hat{P}\right] = 0\,. \tag{51}$$

Hence it clearly implies that parity non-conservation (parity violation) means that its Hamiltonian does not commute with the parity operator $\hat{P}$.

Parity non-conservation (PNC) was discovered in the beta decay of ^{60}Co by Wu and co-workers in 1957 following the prediction by Lee and Yang a year earlier [63]. This lack of mirror symmetry has now been observed in several systems and even in atoms which is an important phenomenon to study. The latest measurement of parity non-conservation in cesium with unprecedented accuracy (0.35%) has led to the discovery of the nuclear anapole moment [64].

The dominant contribution to PNC in atoms comes from the neutral weak current (NWC) interaction between the electron and the nucleus [65]. The effective Hamiltonian describing the interaction consists of two parts, one of which is nuclear spin independent (NSI) [65] and the other is nuclear spin dependent (NSD) [66, 67]. In this review article we will concentrate on NSI parity non-conservation in atoms. The NSI effective Hamiltonian is expressed as

$$H_{PNC} = \frac{G_F}{2\sqrt{2}} Q_W \sum_e \gamma_5^e \rho(r_e), \tag{52}$$

with

$$Q_W = 2\left[ZC_{1p} + NC_{1n}\right]. \tag{53}$$

Here Z and N are the number of protons and neutrons respectively and C_{1p} and C_{1n} are the vector (nucleon) - axial vector (electron) coupling coefficients whereas G_F is the Fermi coupling constant and $\rho(r_e)$ is the normalized nucleon number density. The matrix element of H_{PNC} scales as Z^3 and it has been treated as a perturbation. It is primarily because of this reason that the heavy atoms are considered to be the best candidates for PNC experiments. The total Hamiltonian is now represented by

$$H = H_0 + H_{PNC}. \tag{54}$$

This perturbation causes the wavefunction to take the form $|\Psi\rangle = \left|\Psi^{(0)}\right\rangle + \left|\Psi^{(1)}\right\rangle$, where $\left|\Psi^{(0)}\right\rangle$ and $\left|\Psi^{(1)}\right\rangle$ are the unperturbed and the perturbed part of the wave function respectively.

The quantity that is measured in such an experiment depends on the interference of a parity non-conserving electric dipole transition amplitude ($E1_{PNC}$) and an allowed transition amplitude corresponding to two atomic states of the same parity [68]. From the theoretical point of view an accurate calculation of $E1_{PNC}$ must be based on a suitable and accurate relativistic many-body theory. In a recent review, Ginges and Flambaum [69] have presented the current status of atomic PNC calculations and experiments. A number of many-body theories have been applied to calculate $E1_{PNC}$ matrix elements. The results of these calculations in combination with the most accurate PNC experiment on Cs is in agreement with the Standard Model (SM) of particle physics [69].

Table 8: $E1_{PNC}$ matrix elements for Cs and Ba^+

Atom	Transition	$E1_{PNC}(iea_0(Q_W/-N))$
Cs	$6s\,^2S_{1/2} \longrightarrow 7s\,^2S_{1/2}$	0.910×10^{-11}
Ba^+	$6s\,^2S_{1/2} \longrightarrow 5d\,^4D_{3/2}$	2.05×10^{-11}

We have formulated a new approach to PNC in atoms based on relativistic CC theory in an attempt to go beyond the existing calculations. In this formulation the excitation operators (both T and S) contain an unperturbed (superscript 0) and a perturbed part (superscript 1). For a single valence systems like cesium the wavefunction can be written as

$$|\Psi_k\rangle = \exp(T^0 + T^{(1)}) \left\{1 + S^{(0)} + S^{(1)}\right\} |\Phi_k\rangle \,. \tag{55}$$

This equation follows from Eq.(24) and can be derived easily [70]. The equations for determining $T^{(1)}$and $S^{(1)}$ amplitudes are the following :

$$\langle \Phi^\star | \left[\overline{H}_N, T^{(1)}\right] |\Phi_0\rangle + \langle \Phi^\star | \overline{H}_{PNC} |\Phi_0\rangle = 0 \,, \tag{56}$$

and

$$\left\langle \Phi_v^k \right| \overline{H}_N S_v^{(1)} - \Delta E_v^{(0)} S_v^{(1)} |\Phi_v\rangle + \left\langle \Phi_v^k \right| \overline{H}_N \left\{T^{(1)} + T^{(1)} S_v^{(0)}\right\} + \overline{H}_{PNC} \left\{1 + S_v^{(0)}\right\} |\Phi_0\rangle = 0 \,. \tag{57}$$

The parity non-conserving electric dipole transition amplitude between atomic states $|\Psi_i\rangle = \left|\Psi_i^{(0)}\right\rangle + \left|\Psi_i^{(1)}\right\rangle$ and $|\Psi_f\rangle = \left|\Psi_f^{(0)}\right\rangle + \left|\Psi_f^{(1)}\right\rangle$ is given by

$$E1_{PNC} = \frac{\langle \Psi_f | \vec{D} |\Psi_i\rangle}{\sqrt{\langle \Psi_f | \Psi_f\rangle \langle \Psi_i | \Psi_i\rangle}} \,. \tag{58}$$

The preliminary results we have obtained using this approach are given in table 8. These calculations have been carried out in the Dirac-Coulomb approximation with an universal Gaussian basis consisting of $13s$, $12p$, $11d$ and $7f$ function for Cs and $13p$, $12p$, $11d$ and $8f$ functions for Ba^+. Our results for Cs is in reasonable agreement with linear relativistic CCSD(T) calculation [71] which yields $E1_{PNC} = 0.0908(9) \times 10^{-11}$ in the same units as our calculation.

7 Conclusion

It is clear that considerable progress has been made during the past three decades on the relativistic many-body theory of atoms. However there are some open problems in this field. Perhaps the two areas that deserve most attention is the future are :

(i) Relativistic multi-reference theories to treat a wide variety of open shell heavy atoms including rare-earths. Work in this area is in its infancy [72].

(ii) Incorporation of QED effects in a systematic way in the framework of relativistic many-body theory.

One can indeed look forward to exciting new developments in relativistic electronic structure of atoms in the coming decade.

Acknowledgements : Some of the computations presented in this review were performed on CDAC's Teraflop Supercomputer Param Padma in Bangalore and in our group's Xeon PC cluster which was procured from the BRNS project # 2002/37/12/BRNS. Previous members of our group, in particular, Dr. Angom Dilip Singh, Dr. Holger Merlitz, Dr. Uttam Sinha Mahapatra, Dr. Geetha Gopakumar and Dr. Sonjoy Majumder have made important contributions to our effort on relativistic many-body theory of atoms.

References

[1] B. Swirles, *Proc.Roy. Soc. A*, **152**, 625 (1935).

[2] I. P. Grant, *Proc. Roy. Soc. A*, **262,** 555 (1961)
I. P. Grant, *Adv. Phys.*, **19**, 747 (1970).

[3] J. P. Desclaux, *Comp.Phys.Comm*, **9,** 31 (1975).

[4] I. P. Grant, B.J. McKenzie, P. H. Norrington, D. F. Mayers and N. C. Pyper, Comp. *Phys. Comm*, **21,** 207 (1980).

[5] J. Andriessen, Internal report, *Laboratorium voor Technische Natuurkunde Lorentzweg 1*, Delft, Netherlands, unpublished (1974).

[6] J. Andriessen, K. Raghunathan, S. N. Ray, T. P. Das and D. Ikenberry, *Phys. Rev. A*, **13,** 1669 (1976).

[7] J. P. Desclaux, K. T. Cheng and Y-K. Kim, *J. Phys. B*, **12**, 3819 (1979).

[8] I. P Grant, *Phys. Scr.,* **21**, 443 (1980).

[9] B. P. Das, J. Andriessen, M. Vajed-Samii, S. N. Ray and T. P. Das, *Phys. Rev. Lett.,* **49**, 32 (1982).

[10] T. R. Verhey, B. P. Das and W. F. Perger, *J. Phys. B,* **20,** 3639 (1987).

[11] S. A. Blundell, W. R. Johnson and J. Saperstein, *Phys. Rev.* A, **38**, 4961 (1988).

[12] A. C. Hartley, E. Lindroth and A-M. Martensson-Pendrill, *J. Phys. B,* **23**, 3417 (1990).

[13] J. Sapirstein, *Rev.Mod.Phys.*, **70**, 55 (1998).

[14] U. Kaldor, *Recent advances in Coupled-Cluster Methods*, p 125, Ed. Rodney J. Bartlett, World Scientific, Singapore (1997).

[15] S. A. Blundell, W. R. Johnson and J. Sapirstein, *Phys. Rev. A*, **43**, 3407 (1991).

[16] U. Kaldor, *Lecture Notes in Physics, Microscopic Quantum many-body theories and their applications,* p.71, Eds. J. Navarro and A. Polls, Springer-Verlag-Berlin, Heidelberg and New York (1998).

[17] S. Salomonson and A. Ynnerman, *Phys. Rev. A*, **43**, 88 (1991).

[18] G. Gopakumar, H. Merlitz, R. K. Chaudhuri, B. P. Das, U. S. Mahapatra and D. Mukherjee, *Phys. Rev. A*, **66**, 032505 (2002).

[19] L. Visscher, K. G. Dyall and T. J. Lee, *Int. J. Quant. Chem. Symp.*, **29**, 411 (1995).

[20] L. Visscher, K. G. Dyall and T. J. Lee, *J. Chem. Phys.*, **105**, 8769 (1996).

[21] L. Visscher and K. G. Dyall, *J. Chem. Phys.*, **104**, 9040 (1996).

[22] E. Eliav and U. Kaldor, *Chem. Phys. Lett.*, **248**, 405 (1996).

[23] P. Strange, *Relativistic Quantum Mechanics with applications in condensed matter and atomic physics*, Cambridge University Press, London (1998).

[24] R E. Stanton and S. Havriliak, *J. Chem Phys*, **81**, 1910 (1984).

[25] A. K. Mohanty and E. Clementi, *Chem. Phys. Lett.*, **157**, 348 (1989).

[26] A. D. McLean and Y. S. Lee, *J. Chem. Phys.*, **76**, 735 (1982).

[27] Y. Ishikawa, R. C. Binning and K. M. Sando, *Chem. Phys. Lett.*, **101**, 111 (1983).

[28] K. G. Dyall, I. P. Grant and S. Wilson, *J. Phys. B*, **17**, 493 (1984).
K. G. Dyall, I. P. Grant and S. Wilson, *J. Phys. B*, **17**, 1201 (1984).
K. G. Dyall, I. P. Grant and S. Wilson, *J. Phys. B*, **17**, L45 (1984).

[29] G. Breit, *Phys. Rev.*, **34**, 353 (1929).
G. Breit, *Phys. Rev.*, **36**, 363 (1930).

[30] H. M. Quiney, I. P. Grant and S. Wilson, *J. Phys. B*, **20**, 1413 (1987).

[31] L. N. Labzowsky, G. L. Klimchitskaya and Y. Y. Dmitriev, *Relativistic Effects in the Spectra of Atomic Systems*, Institute of Physics Publishing Ltd., Britstol (1993).

[32] T. Beier, *Phys. Rep.*, **339**, 106 (2000).

[33] A. M. Desiderio and W. R. Johnson, *Phys. Rev. A*, **3**, 1267 (1971).

[34] V. M. Shabaev, *Phys. Rep.*, **356**, 119 (2002).

[35] R. F. Bishop, *Lecture Notes in Physics, Microscopic Quantum many-body theories and their applications,* p.1, Eds. J. Navarro and A. Polls, Springer-Verlag-Berlin, Heidelberg and New York (1998).

[36] R. J. Bartlett, *Modern Electronic Structure Theory*, vol-II, p.1047, Ed. D. R. Yarkony, World Scientific, Singapore (1995).

[37] I. Lindgren and J. Morrison, *Atomic Many-Body Theory* (Springer, Berlin) 1985.

[38] N. C. Pyper, *J. Phys. B*, **16**, L211 (1983).

[39] C. Froese Fischer, *J. Phys. B*, **16**, 151 (1983).

[40] D. Frye, S. Lakdawala and L. Armstrong Jr., *Phys. Rev. A*, **27**, 1709 (1983).

[41] B.P. Das, J. Hata and I.P. Grant, *J. Phys. B*, 17, L1 (1984).

[42] I.P. Grant, *Advances in Physics*, 19 (1970).

[43] L. I. Schiff, *Phys. Rev.*, **132**, 2194 (1963).

[44] P. G. H. Sandars, *Phys. Lett.*, **14**, 194 (1965).
P. G. H. Sandars, *Phys. Lett.*, **22**, 290 (1966).

[45] Alok Shukla, B. P. Das and J Andreissen, *Phys. Rev. A*, **50**, 1155 (1994).

[46] Alok Shukla, B. P. Das and D. Mukherjee, *Phys. Rev. A*, **50**, 2096 (1994).

[47] M. Yu Kuchiev, V. V. Flambaum, *J. Phys. B*, **36**, R191 (2003).

[48] Z. W. Liu, H. P. Kelly, *Phys. Rev. A*, **45**, R4210 (1992).

[49] B. P. Das, *Lecture Notes in Chemistry,* p. 411, Ed. D. Mukherjee, Springer-Verlag, Berlin (1989).

[50] A. M. Martensson-Pendrill and E. Lindroth, *Euro. Phys. Lett.*, **15**, 155 (1991).

[51] R. K. Chaudhuri, P. K. Panda and B. P. Das, *Phys. Rev. A*, **59**, 1187 (1999).

[52] R. C. Raffenetti and K. Ruedenberg, *J. Chem. Phys.*, **59**, 5978 (1973).

[53] K. T. Cheng and W. J. Child, *Phys. Rev. A*, **31**, 2775 (1985).

[54] I. Lindgren and A. Rosen, *Case Stud. At. Phys.*, **4**, 197 (1974).

[55] S. Majumder, G. Gopakumar, H. Merlitz and B. P. Das, *J. Phys. B.*, **34**, 1 (2001).

[56] C. Sur, B. K. Sahoo, R. K. Chaudhuri, B. P. Das and D. Mukherjee, To be published in *Eur. Phys. J. D* (2004).

[57] B. K. Sahoo, G. Gopakumar, R. K. Chaudhuri, B. P. Das, H. Merlitz, U. S. Mahapatra, and D. Mukherjee, *Phys. Rev. A*, **68**, 040501 (R) (2003).

[58] S. Ahmed, J. Andriessen and T. P. Das, *Phys. Rev. A*, **27**, 2790 (1983).

[59] M. S. Safronova, W. R. Johnson and A. Derevianko, *Phys. Rev. A*, **58**, 1016 (1998).

[60] S. Ahmad, J. Andriessen, K. Raghunathan and T. P. Das, *Phys. Rev. A*, **25**, 2923 (1982).

[61] Xin Feng, Guo-Zhong Li, R. Alheit, and G. Werth, *Phys. Rev. A*, **46**, 327 (1988).

[62] B. K. Sahoo, R. K. Chaudhuri, B. P. Das, H. Merlitz and D. Mukherjee, Submitted to *Phys. Rev. Lett.* (2004).

[63] C. S. Wu, E. Ambler, R. W. Hayward and R. P. Hudson, *Phys. Rev.*, **105**, 1413 (1957).

[64] C. S. Wood *et al*, *Science*, **275**, 1759 (1997).

[65] E. D. Commins and P. H. Bucksbaum, *Weak Interactions in Quarks and Leptons*, Cambridge University Press, London (1983).

[66] V. V. Flambaum and I. B. Khriplovich, *Zh. Esp. Teor. Fiz*, **79**, 1656 (1980). [*Sov. Phys. JETP*, **52**, 835 (1980)].

[67] C. Bouchiat, *Z. Phys. C*, **49**, 91 (1991).

[68] D. N. Stacey, *Phys. Scr.*, **T40**, 15 (1992).

[69] J. S. M. Ginges and V. V. Flambaum, *Phys. Rep.*, **397**, 63 (2004).

[70] K. P. Geetha, *Ph.D Thesis*, Bangalore University (2001).

[71] S. A. Blundell, W. R. Johnson, and J. Sapirstein, *Phys. Rev. Lett.*, **65**, 1411 (1990).

[72] M. J. Vilkas and Y. Ishikawa, *Phys. Rev. A*, **69**, 062503 (2004).